Using Soya Flour as an Eco-Friendly Filler to Partially Replace Carbon Black in Tire Tread Compounds

B.V.S.N. Bopeththa[1], H.N.A.B. Abeygunawardana[1], T.D. Kuruwita Mudiyanselage[1*], and D.M.R.K. Gunarathne[2]

[1]Department of Polymer Science, Faculty of Applied Sciences, University of Sri Jayewardenepura, Sri Lanka
[2]Innovation and Technology Department, Trelleborg Lanka Pvt. (Ltd.), Levin's Drive, Sapugaskanda, Makola, Sri Lanka

Date Received: 31-01-2025 Date Accepted: 28-06-2025

Abstract

Adapting to sustainable materials is now prevalent in many industries, including the tire industry. Several biomaterials have been utilized at various stages of tire development for their sustainability. This endeavor highlights the utilization of soy flour (SF) for partial replacement of petroleum-based carbon black (CB) in tire tread compounds. SF had an average moisture percentage of 6.74%. SF successfully replaces 10 phr of CB without major loss in physical properties. It exhibits a tensile strength of 19.59 MPa, an elongation at break of 588.43%, a 300% modulus of 5.14 MPa, a Shore A hardness of 51, a specific gravity of 1.093, and a resilience of 54%. Additionally, SF shows an abrasion value of 277.74 mm^3, a tear strength of 34.36 N/mm, and an adhesion strength of 7.60 N/mm. Further, SF displayed properties comparable to the control with a silane coupling agent, and calcium sulfate dihydrate (CSD). However, SF with CSD led to a higher abrasion loss (approximately 60% improvement over the control), which indicated a less favorable interaction between SF and NR. Despite this difference, all formulations demonstrated acceptable performance in aging and blooming tests. Therefore, it can be clearly concluded that SF together with a silane coupling agent could easily replace 10 phr of CB, serving as sustainable filler in the tire manufacturing industry.

Keywords: *Eco-friendly, Filler, Tire tread, Soya flour, Carbon black*

**Correspondence: thilinidg@sjp.ac.lk*

1. Introduction

Tires are fundamental components of vehicles, providing critical functions such as traction, stability, and safety, while simultaneously contributing to fuel efficiency and overall vehicle performance. The tire tread compound, a key element of tire construction, directly influences the tire's functionality, longevity, and safety. Serving as the interface between the vehicle and the road, the tread compound is designed to optimize performance under diverse conditions, including wet, dry, and icy surfaces. Its formulation must strike a balance between durability, elasticity, and abrasion resistance, ensuring the tire's reliability throughout its lifespan. In Sri Lanka, the tire industry benefits from the availability of natural rubber (NR), a renewable resource that plays a pivotal role in the region's tire manufacturing sector (Boonmahitthisud and Boonkerd, 2021). The abundance of NR in Sri Lanka offers a strategic advantage, positioning the country as a key supplier in the global tire market. With global tire production exceeding 2.2 billion units annually, even modest improvements in sustainability within the sector could yield significant environmental benefits (Tire Market: The Global Tire Industry Analysis, Report ID: SR112023A575).

In tire manufacturing, various additives are incorporated into the rubber compound to enhance the performance, durability, and processing efficiency of the final product. Despite NR's inherent sustainability, conventional tire manufacturing depends heavily on different petroleum-based additives. A primary additive, carbon black (CB) is a reinforcing filler to enhancing durability (Chakraborty, 2024), strength (Ismail et al., 2011), and abrasion resistance (Fan et al., 2020) of tires. Plasticizers and processing oils such as paraffinic and naphthenic oils (Susanto, 2018) are used to increase the flexibility (Wypych, 2004) of the rubber, allowing for easier processing (Petchkaew, 2015) during the production stages. Antioxidants like phenolic compounds (Rodgers and Waddell, 2005) or amines (Xu et al., 2022) are added to prevent oxidative degradation (Pisoschi and Pop, 2015), which can cause the rubber to harden or crack over time, thereby extending the tire's lifespan. Curing agents, most notably sulfur, are essential in the vulcanization process, where sulfur (Innes et al., 2024) forms cross-links between the rubber molecules, improving the elasticity and strength of the tire. Apart from CB, silica is also a common reinforcing filler that contributes to improving the tire's tread wear resistance (Sarkawi et al., 2015), fuel efficiency (Neethirajan et al., 2022), and wet traction (Bera et al., 2024). The careful selection and balance of these additives are vital in optimizing tire performance, ensuring safety, and meeting environmental standards. Petroleum-based additives such as CB and oils are widely used due to their capacity to reinforce rubber; yet, they present serious environmental and health concerns (Niranjan and Thakur, 2017). The CB is produced via incomplete combustion of heavy petroleum, a process that releases considerable amount of carbon dioxide (Huang et al., 2022) and particulate matter, exacerbating both climate change and respiratory health risks in manufacturing communities. Additionally, CB particles are environmentally persistent, leading to long-term ecological accumulation (Schmidt and Noack, 2000). Alternative fillers, like silica (Rostami-Tapeh-Esmaeil et al., 2023), have been explored to address these concerns; however, they are costly and require energy-intensive processing. However, the production and disposal of tires present significant environmental challenges (Formela, 2021), primarily due to their reliance on petroleum-based materials and the complex processes required for tire recycling. As awareness of sustainability issues intensifies globally, the tire industry is undergoing a transformative shift, with increased emphasis on reducing environmental impact and improving resource efficiency through material innovations and cleaner production methods (Bijina et al., 2023). While biodegradable fillers and agricultural waste (Koriem et al., 2023) show promise, these alternatives have yet to achieve the performance and compatibility required for widespread industrial application, highlighting a critical gap in sustainable tire additives.

Different biomaterials have been utilized for rubber compounding, and their effect on final properties investigated. Bhadra and co-workers used a range of virgin biomaterials such as maize starch, wheat starch, rice starch, cassava starch, MCC, CMC, lignin, and soya flour (SF) as fillers

*Correspondence: thilinidg@sjp.ac.lk

compared to the silica-filled in SBR and BR tire tread compound as the control sample (Bhadra et al, 2019). Other researchers (Kosikova et al, 2007) have mixed lignin (ranging from 10 to 30 phr) with NR and observed a reduction in thermo-oxidative degradation in air and further studied the applicability of lignin material with SBR. Defatted soya flour (DSF) was used with SBR latex to make an elastomer composite (Jong, 2005) of which the tensile strength was improved to certain strained values, but elongation at break value had decreased. The author (Jong, 2007) had used a co-filler of CB and soya spent flakes (SSF) to make a composite with SBR latex which showed a 100% improvement of shear elastic modulus than the unfilled elastomer.

SF has a range of molecular weight from 8 kDa to 600 kDa (8 g mol^{-1} to 600 g mol^{-1}). A possible high rigidity value in the reinforcement phase is one of the requirements of rubber reinforcement. The reported shear elastic modulus for dry soya protein is about 2 GPa at ambient conditions (Jong, 2005). Therefore, dry soya protein is an attractive candidate for rubber reinforcement.

This study introduces SF as a novel, bio-based filler to partially replace CB in tire tread compounds; it is noteworthy that this concept has not been previously explored in tire manufacturing. Different SF to CB ratios has been tested over mechanical and physical properties. The results revealed that partial replacement of CB with SF is possible without any significant property loss. This investigates SF as a partial CB substitute, presenting a pioneering bio-based filler solution for tire production that may significantly reduce environmental impact without compromising critical performance standards.

2. Methodology

2.1 Materials

Industrial grade chemicals were used in this work. Natural rubber, carbon black, silica, silane coupling agent, sulfur, activators, accelerators, retarders, antioxidants, and processing oil were supplied by Trelleborg Lanka (Pvt.) Ltd., Makola, Sri Lanka. Soya flour was purchased from a local supplier in Matale, Sri Lanka. Industrial grade $CaSO_4 \cdot 2H_2O$ was bought from Rohanlack, Dyes and Chemicals, Sri Lanka.

2.2 Rubber Compound formulations

Firstly, the possibility of replacing CB with SF with (without silane coupling agent) was investigated as given in Table 1. Dried SF sample was manually sieved using a mesh (80 mesh size/170 μm) to obtain the consistent fine particles for compounding. Based on the results, the second stage was carried out with silane coupling agents and the compatibilizer CSD to increase the coupling between the SF and NR. The formulations are tabulated in Table 2.

Silane was used as a coupling agent (CA) to improve the compatibility between silanized filler (SF) and natural rubber (NR). In industrial practice, silane is typically added at a 1:10 ratio to silica fillers to enhance the interaction with elastomers (Barrera Torres et al., 2021). Following this approach, silane was added in a 1:10 ratio to SF during the preparation of SF10(SI). For SF15(SI)R, 1.5 phr of silane was used, maintaining the same 1:10 ratio with SF. However, in SF15(SI), the same amount of silane as in SF10(SI) was used to control costs and avoid the expense of additional silane.

Table 1: Initial compound formulations

Material	Unit	Sample ID:		
		S0	SF10	SF10(SI)
NR	Phr	100	100	100
Carbon Black	Phr	50	40	40
Silane	Phr	0	0	1
(SF) Soya filler	Phr	0	10	10

*Correspondence: thilinidg@sjp.ac.lk

Table 2: The compound formulations of the second stage

Material	Unit	Sample ID:				
		S0	SF15(SI)	SF10-CSD	SF10(SI)-CSD	SF15(SI)_R
NR	Phr	100	100	100	100	100
Carbon Black	Phr	50	35	40	40	35
Silane	Phr	0	1	0	1	1.5
(SF) Soya filler	Phr	0	15	10	10	15
CSD ($CaSO_4 \cdot 2H_2O$)	Phr	0	0	0.5	0.5	0

2.3 Preparation of the master batch

The standard procedure on preparing the master batch was followed. General tire formulation was utilized. Reference (S0) and sample were developed according to the sated formulations in Tables 1 and 2.

2.4 Testing and characterization

The cure characteristics of the compounds were measured by rubber process analyzer at 151 ºC for 30 min. Physical and mechanical properties of the samples were analyzed from Tensile, Tear, Hardness, SPG (Specific gravity), Resilience, Abrasion, Flexometer, Adhesion, and Carbon black dispersion (CB dispersion test) tests. All the tests were conducted according to ASTM standards provided by alfa-technologies (U.K.). The aging test was performed by measuring tensile properties of the aged samples at 100 ºC for 01 day and for 03 days, and 70 ºC for 07 days. The Blooming test was performed using square-shaped test samples both indoors and outdoors. Images of each test sample of each trial were taken by a digital camera. Indoor experiments were conducted at the laboratory, and for the outdoor experiments, the samples were placed in a natural environment where ample sunlight could be obtained daily.

3. Results and Discussion

3.1 Cure Characteristics

The Moving Die Rheometer (MDR) test was performed to evaluate the cure characteristics of the formulations in the context of the production process. ML values, which represent the minimum torque observed during mixing and correspond to the compound's lowest viscosity, are presented in Figure 1(a). Lower ML values indicate improved processability and reduced energy requirements during mixing, translating to potential cost savings in production. The results show that the ML values for SF10, SF15(SI), and SF15(SI)_R are comparable to the control sample. In contrast, formulations SF10(SI), SF10-CSD, and SF10(SI)-CSD exhibit higher ML values than the control. These findings suggest that formulations with lower amount of SF without a coupling agent (CA) or higher amount of SF with CA achieve similar viscosity levels as to the control. However, formulations with lower SF combined with CA demonstrate higher viscosities, indicating stronger interactions between the SF and the elastomer in the presence of CA. This enhanced interaction is likely to be responsible for the increased ML values observed in the graph. These results highlight the influence of CA and SF phr levels on the processability and energy demands of the compound formulations.

*Correspondence: thilinidg@sjp.ac.lk

When considering MH values (Figure 1(a) of SF10, SF10-CSD, SF10(SI)-CSD, and SF15(SI)_R show comparable values with the MH of the control. MH of SF10(SI) is higher and SF15(SI) is lower than the control. The trial SF10(SI) shows a higher MH value revealing that it has higher filler-rubber crosslinking density (FRCD), and SF15(SI) shows lower FRCD. When the SF amount increases, FRCD becomes lower if it contains CA. Shear viscous stress (S”) is the friction activated between consecutive fluid layers. It is somewhat of a similar property to the torque. In this study, S" values at ML and MH follow a pattern similar to that of the reference, except for SF15(SI)_R (Figures 1(b) and 1(c)). Both SF10(SI) and SF15(SI) exhibit relatively lower S" values at MH. For SF10(SI), the SF was introduced by partially replacing carbon black (CB) without using a CA. The absence of CA likely caused SF particles to aggregate due to inadequate dispersion, hindering effective crosslinking between rubber chains. This resulted in lower MH and reduced S" at MH. Similarly, the lower S" at MH in SF15(SI) can be attributed to the higher SF content, which exacerbates the aggregation issue. Conversely, SF15(SI)_R displays an unexpected increase in S" at MH, which cannot be explained by the observed MH value, suggesting the presence of an unidentified interaction or mechanism.

The cure extent and cure rate, determined using the Moving Die Rheometer (MDR) test, are shown in Figures 1(d) and 1(e). SF10(SI) demonstrates a slight increase in cure extent, possibly due to the formation of a highly structured SF-NR crosslink network facilitated by silane. Other formulations exhibit cure extents comparable to the control. The cure rate index (CRI) data in Figure 1(e) reveals reductions in SF10(SI), SF15(SI), SF10(SI)-CSD, and SF(SI)_R, potentially due to the impact of silane on sulfur crosslinking. However, SF10-CSD shows an improved CRI, which could be attributable to the addition of CSD, as it does not interfere with sulfur crosslinks during the curing process. The MDR test results at 151 °C for 30 minutes suggest that all tested formulations are viable for use in tread compound applications relative to the control. However, higher ML values observed in SF10(SI), SF10-CSD, and SF10(SI)-CSD indicate greater energy absorption during the mixing process, which represents a drawback for these formulations.

3.2 Mechanical properties

3.2.1 Tensile Strength

Tensile strength is a critical mechanical property of rubber compounds, especially in tire applications. As shown in Figure 2(a), SF10(SI) and SF10-CSD exhibit comparable tensile strength to the control sample, while other samples show slightly lower values. In SF10, replacing CB with SF reduces tensile strength, indicating lower compatibility of SF with NR compared to CB. However, the use of silane and CSD in SF10(SI) and SF10-CSD enhances tensile strength, suggesting improved compatibility between SF and NR. Notably, in SF15(SI), increasing the SF content while incorporating silane leads to a reduction in tensile strength, confirming that higher SF levels negatively affect this property. SF10(SI)-CSD and SF15(SI)_R show even lower tensile strength, potentially due to filler aggregation caused by excessive CA. The aggregation likely arises from interactions between SF, silane, and CSD, which promote clustering rather than dispersion.

Despite these variations, the tensile strength differences across trials are minor enough to conclude that replacing 10 phr of CB with SF does not significantly impact the material's tensile strength. Under aging conditions (100 ºC for 1 day, 100 ºC for 3 days, and 70 ºC for 7 days), the tensile strength variations remain consistent with the normal state. After 1-day aging at 100 ºC, the control sample shows negligible deterioration, whereas SF10 exhibits higher deterioration, which decreases with the addition of silane or CSD. Increasing CA content further reduces tensile strength in SF10(SI)-CSD and SF15(SI)_R due to filler aggregation. After 3-day aging at 100 ºC, all samples show a deterioration of approximately -40%. At 70 ºC for 7 days, no significant deterioration is observed, with some samples even showing improved tensile strength, possibly due to post-curing at lower temperatures.

The aging behavior of SF10(SI), SF15(SI), SF10-CSD, and SF10(SI)-CSD is comparable to the control sample, demonstrating acceptable performance under these conditions.

*Correspondence: thilinidg@sjp.ac.lk

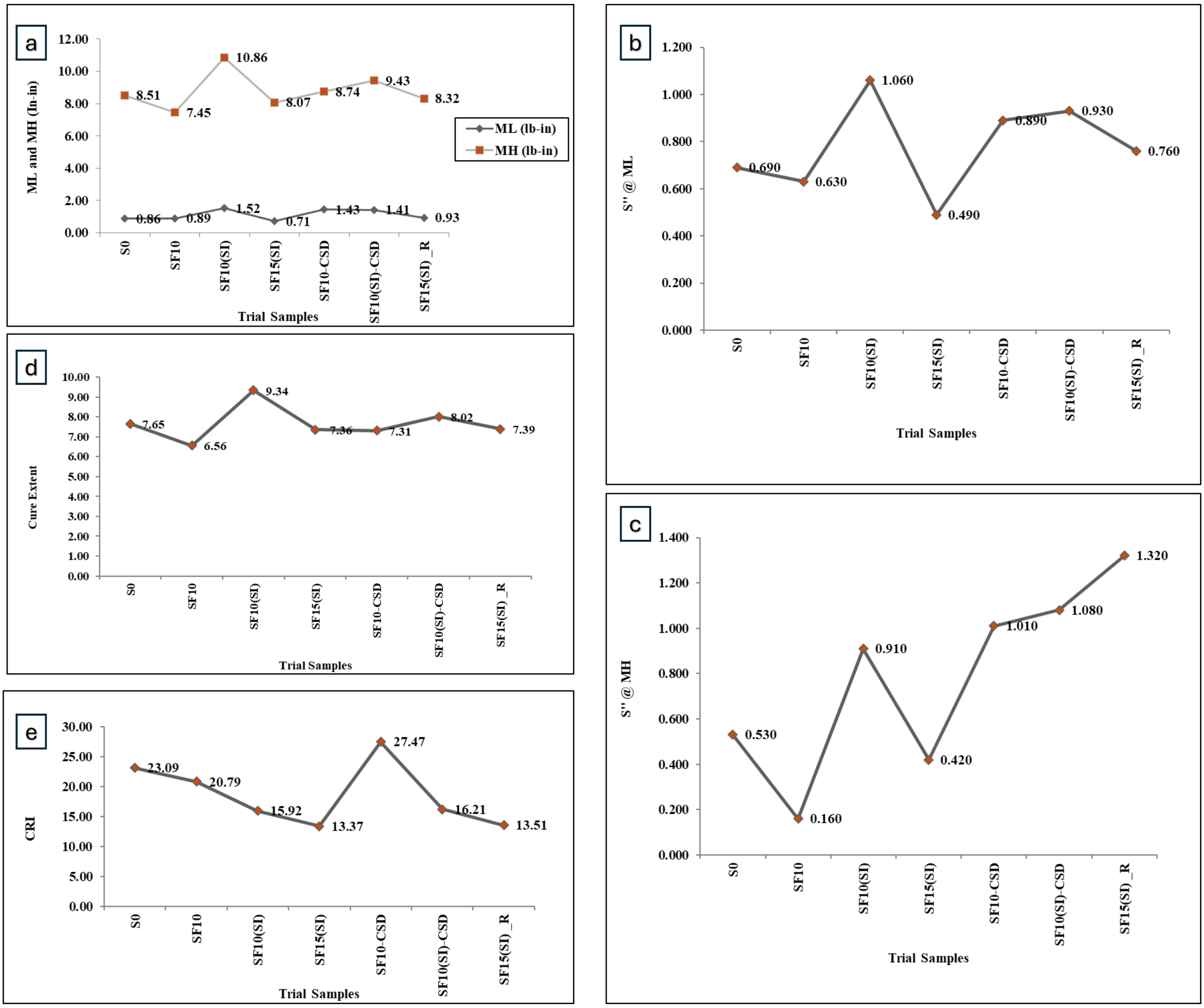

Figure 1: (a) The graph of ML and MH (lb-in) vs. trial samples (at 151 ºC for 30 min) **(b)** The graph of S" at ML vs. trial samples (at 151 ºC for 30 min) **(c)** The graph of S" at MH vs. trial samples (at 151 ºC for 30 min) **(d)** The graph of cure extent vs. trial samples (at 151 ºC for 30 min) **(e)** The graph of CRI vs. trial samples (at 151 ºC for 30 min)

3.2.2 Elongation at Break (PEB)

Figure 2(b) indicates that the control and SF10 trials exhibit similar PEB values, while other samples show slightly lower values due to the addition of CAs. The inclusion of CAs promotes crosslinking between SF and NR, resulting in higher crosslink density (FRCD). This increased density reduces the molecular weight between crosslink points, leading to stiffer material with reduced elongation capacity. The variations in PEB among trials range from 0% to -18%, which are acceptable since they remain within the -20% threshold. SF10 exhibits minimal changes compared to the control.

Under aging conditions, PEB variations are similar to those observed under normal conditions. After 1-day aging at 100 ºC, the control sample shows an 11.93% reduction, while SF10 experiences

*Correspondence: thilinidg@sjp.ac.lk

a higher reduction (25.24%). Adding silane or CSD mitigates this deterioration. For 3-day aging at 100 ºC, PEB reductions for all samples range from -25% to -38%, with SF10 showing unexpectedly low deterioration (-28.21%), likely due to experimental error. For 7-day aging at 70 ºC, the trend resembles that of 1-day aging at 100 ºC, with SF10(SI), SF15(SI), and SF10-CSD showing lower PEB deterioration.

3.2.3 Modulus at 300% Elongation (M300)

Figure 2(c) shows that SF10 has a lower M300 than the control, indicating reduced compatibility and adhesion between SF and NR. Adding silane to SF (SF10(SI)) significantly increases M300, with other samples (SF10(SI) to SF15(SI)-CSD) showing comparable values due to the consistent use of silane or CSD. However, SF15(SI) exhibits slightly lower M300 due to the higher SF content and reduced adhesion. SF10 is the only sample with a significant M300 reduction (-26%), making it the least compatible.

Under aging conditions, M300 variations mirror the normal state, except for SF10-CSD at 100 ºC for 3 days. Post-curing during aging typically increases crosslink density, improving modulus. SF10(SI) exhibits comparable or lower deterioration than the control, suggesting acceptable aging performance.

3.2.4 Hardness

Hardness, measured at low strain levels, reflects material stiffness. Figure 2(d) demonstrates that all trials have similar hardness to the control (50 Shore A), with values ranging from 50 to 55 Shore A. Replacing CB with SF does not significantly alter hardness, indicating that SF contributes adequate stiffness. A gradual increase in hardness from S0 to SF15(SI)-CSD is observed, attributed to improved filler-rubber crosslinking density (FRCD) due to CA addition. Particle size and curing agent levels do not contribute to this increase, as they remain unchanged.

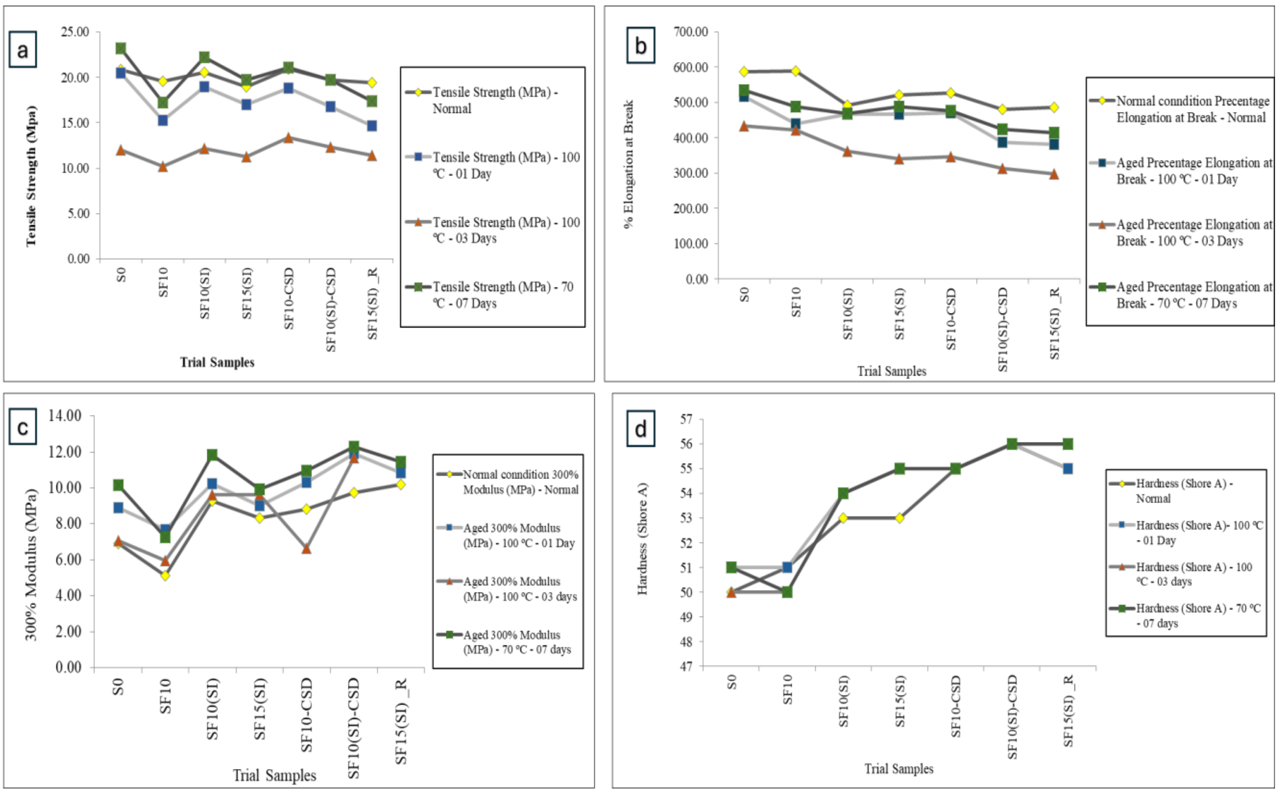

Figure 2: (a) The graph of tensile strength vs. trial sample at different conditions (normal and aging) **(b)** The graph of percentage elongation at break vs. trial sample under different conditions (normal and

*Correspondence: thilinidg@sjp.ac.lk

aging) **(c)** The graph of modulus at 300% elongation vs. trial sample at different conditions (normal and aging) **(d)** The graph of hardness vs. trial sample at different conditions (normal and aging)

Under aging conditions, hardness variations are minimal, with most trials showing no significant deterioration. While SF10 shows slight negative changes in hardness under 1-day and 3-day aging at 100 ºC, the changes are negligible (<2%). Aging typically increases hardness due to post-curing, which enhances crosslink density. Overall, no distinct trends in hardness values are observed, and all trials exhibit acceptable performance.

3.3. Specific Gravity

The specific gravity (SPG) of rubber compounds is an important parameter to maintain within an acceptable range. SPG helps determine the mass of the compound required for curing based on the mold volume. To ensure proper molding, the SPG value must match the mold's volume requirements. The control sample shows the highest SPG, while the other samples exhibit slightly lower but comparable SPG values. This is because the SPG of silica filler (SF) is lower than carbon black (CB). Replacing 10 phr of CB with SF reduces the overall SPG.

Figure 3(a) illustrates the SPG values under different aging conditions (100 °C for 1 day, 100 °C for 3 days, and 70 °C for 7 days). The trends indicate that the SPG variations under aging conditions are similar to those observed under normal conditions.

3.4 Resilience

Resilience or rebound indicates the elasticity of rubber compounds. It is defined as the ratio of energy released during recovery to the energy absorbed during deformation. Figure 3(b) shows that the control sample and SF10 have the highest resilience, while other samples display lower values. Compounds with CA, such as silane or calcium stearate (CSD), increase filler-rubber crosslink density (FRCD), which leads to higher energy loss during recovery and thus lower resilience. Resilience generally behaves inversely to hardness since higher crosslink density improves hardness but reduces resilience. SF15(SI) shows a slight resilience increase, possibly due to the addition of 15 phr SF without an increase in CAs. However, SF15(SI)_R, which contains high SF and CA levels, shows reduced resilience. All resilience variations fall within a -2% to -18% range compared to the control, indicating that the results are acceptable. Samples SF10, SF10(SI), and SF15(SI) demonstrate comparatively good resilience values.

Figure 3(b) also shows resilience variations under aging conditions (100 °C for 1 day, 100 °C for 3 days, and 70 °C for 7 days). Resilience under low aging conditions (100 °C for 1 day or 70 °C for 7 days) does not change significantly. Resilience increases due to enhanced rubber-rubber crosslink density (RRCD) during post-curing. However, resilience deteriorates significantly at 100 °C for 3 days, likely due to chain scission, where long rubber chains break into smaller ones, reducing elasticity and resilience. Despite these changes, all resilience variations remain within ±10%, indicating acceptable performance.

3.5 Abrasion loss

Abrasion loss measures the mass loss of rubber compounds due to friction during sliding. Figure 3(c) shows that replacing CB with SF increases abrasion loss significantly. This is attributed to the larger particle size of SF compared to CB and the lower compatibility between SF and natural rubber (NR). Larger particles have lower specific surface areas, leading to weaker filler-polymer interactions and increased abrasion loss. Adding silane to SF10(SI) reduces abrasion loss, making it comparable to the control. However, higher SF levels in SF15(SI) increase abrasion loss, as do additional amounts of silane and CSD in SF15(SI)_R. Improper mixing of CSD may also cause SF aggregation, worsening dispersion and increasing abrasion loss. Abrasion loss is critical for tire tread materials. Among the

*Correspondence: thilinidg@sjp.ac.lk

samples, only SF10(SI) shows an acceptable reduction (14.94%, below 20%). Other trials exhibit unacceptable abrasion loss increases. Figure 3(c) also depicts abrasion loss under aging conditions (100 °C for 1 day, 100 °C for 3 days, and 70 °C for 7 days). No clear trends are observed between aging conditions, but variations are similar to those under normal conditions.

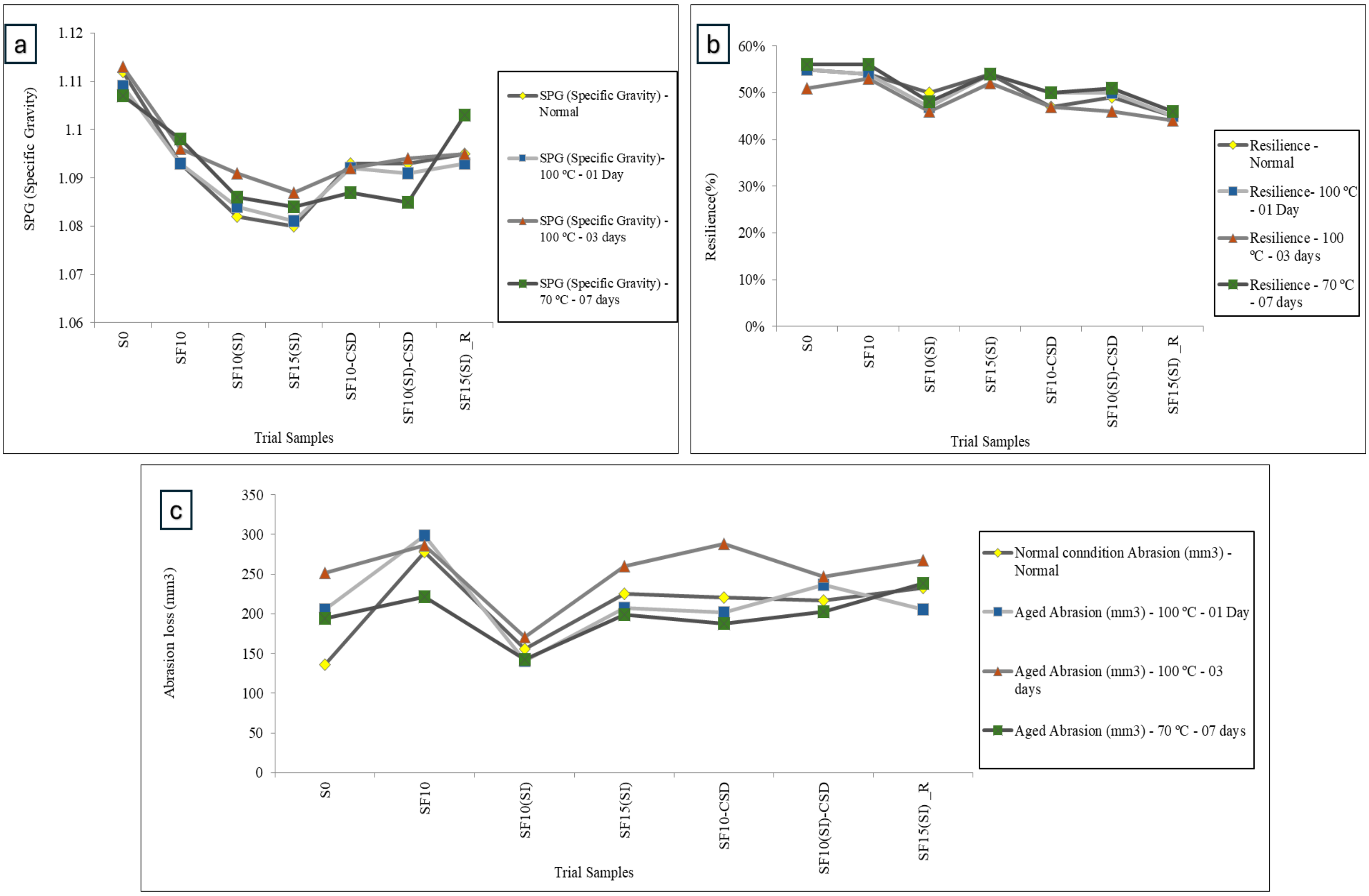

Figure 3: (a) The graph of specific gravity vs. trial sample at different conditions (normal and aging) **(b)** The graph of resilience vs. trial sample at different conditions (normal and aging**) (c)** The graph of abrasion loss vs trial sample at different conditions (normal and aging)

3.6 Blooming Test

Blooming is white coloured dust or patches observed on the surface of rubber compounds when they have bloomed in the environment for a certain period. Probably migration of some additive materials onto the surface of rubber compounds could be the reason for this observation.

3.6.1 Indoor blooming test

Images of test pieces (compound sheets) before and after the indoor blooming test are shown in Table 3. No significant difference cannot be observed visually, which means that adding SF does not affect the blooming under indoor conditions.

*Correspondence: thilinidg@sjp.ac.lk

Table 3: Tabulated images (digital camera images) of the surface of the test pieces before and after the outdoor blooming test

	Sample ID:	**Start**	**End**
Indoor	**S0**		
	SF10		
	SF10(SI)		
	SF15(SI)		

*Correspondence: thilinidg@sjp.ac.lk

SF10-CSD		
SF10(SI)-CSD		
SF15(SI) _R		

3.6.2. Outdoor blooming test

Images of test pieces (compound sheets) before and after the outdoor blooming test are shown in Table 4. According to the images taken, significant differences cannot be identified on samples. Thus, adding SF does not affect the blooming under outdoor conditions.

*Correspondence: thilinidg@sjp.ac.lk

Table 4: Images (digital camera images) of the surface of test pieces before and after the outdoor blooming

	Sample ID:	Start	End
Outdoor	**S0**		
	SF10	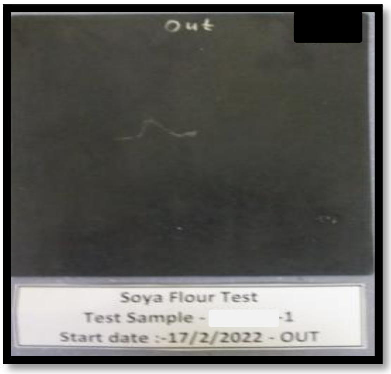	
	SF10(SI)	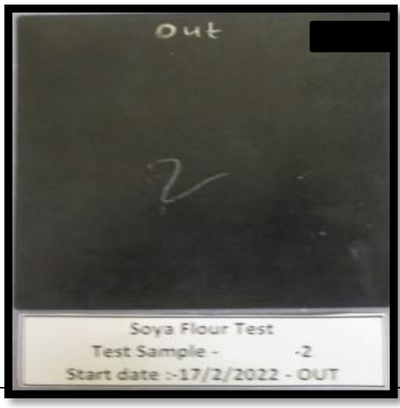	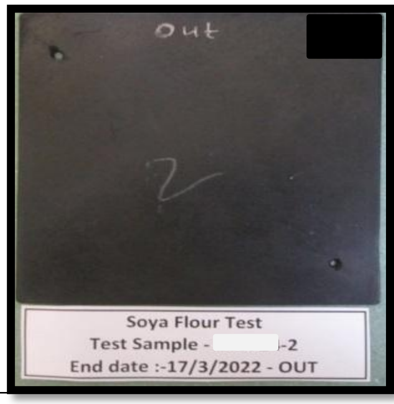
	SF15(SI)		

*Correspondence: thilinidg@sjp.ac.lk

<table>
<tr><td></td><td>SF10-CSD</td><td></td><td>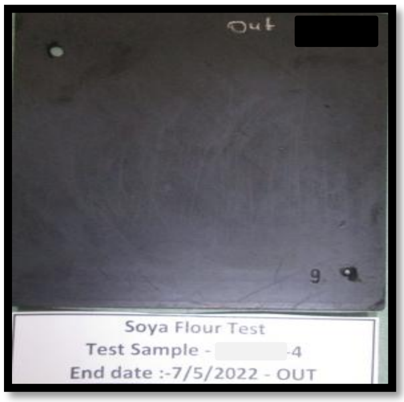</td></tr>
<tr><td></td><td>SF10(SI)-CSD</td><td>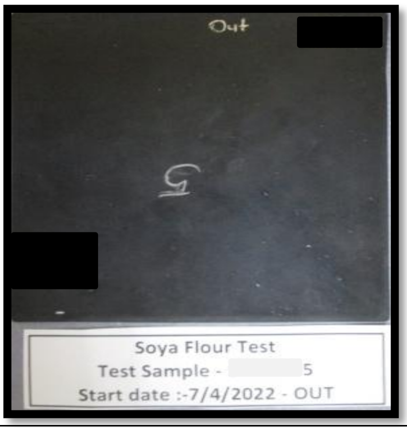</td><td></td></tr>
<tr><td></td><td>SF15(SI)_R</td><td>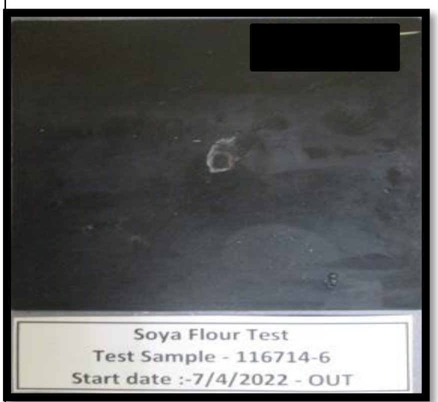</td><td></td></tr>
<tr><td></td><td></td><td></td><td></td></tr>
</table>

3.7 Flexometer heat build-up test

The Flexometer heat build-up test was conducted on the selected formulation, SF10(SI), which demonstrated superior performance in curing, mechanical, and aging properties. Table 5 presents the heat build-up data for SF10(SI), which displayed a marginally higher value than the control sample. Heat build-up is inversely related to thermal conductivity, with higher values indicating lower conductivity.

The increase in heat build-up observed in SF10(SI) can be attributed to the lower intrinsic thermal conductivity of silica (SF) compared to carbon black (CB), as well as the reduced filler-rubber crosslink density (FRCD) stability at elevated temperatures. Although silane enhances crosslinking between SF and natural rubber (NR), these interactions primarily involve weak, non-covalent bonds. At elevated temperatures, these low-energy interactions are prone to dissociation, leading to a decrease

*Correspondence: thilinidg@sjp.ac.lk

in FRCD stability and, consequently, thermal conductivity. The observed increase in heat build-up remains below 20% compared to the control, which is within acceptable limits and does not significantly compromise the performance of the material.

Table 5: Heat build-up and probe temperature values of the S0 and SF10(SI)

Trial No:	Parameter					
	Base Temperature (ºC)		Heat build-up (ºC)	Changing Factor (Heat build-up)	Probe Temperature	Changing Factor (Probe Temperature)
	Start	Final				
S0	93.00	104.00	11.00	-	112.64	-
SF10(SI)	93.00	93.00	13.00	18.18%	124.73	10.73%

3.8 Adhesion strength

Adhesion strength testing was performed to evaluate the compatibility between the prepared tire tread compound and the base compound. Similar to the heat build-up test, the analysis focused on SF10(SI) and the control. As shown in Table 6, SF10(SI) exhibited a 4.59% improvement in adhesion strength over the control sample. The replacement of 10 phr CB with SF in the presence of silane did not compromise adhesion strength. Instead, the improvement suggests effective filler-rubber interactions mediated by silane, which enhanced compatibility between SF and NR. This result supports the suitability of SF10(SI) for tire tread applications.

Table 6: Adhesion strength values of the S0 and SF10(SI)

Trial No:	Adhesion Strength (N/mm)	Changing Factor
S0	7.30	-
SF10(SI)	7.60	4.59%

3.9 Carbon black dispersion test

The results of the carbon black (CB) dispersion test are illustrated in Figure 4(a), revealing that all trials demonstrated lower dispersion compared to the control. Among the experimental formulations, SF10 and SF10(SI) exhibited the highest CB dispersion. The improved dispersion in SF10(SI) is attributed to the relatively low SF content and the action of silane, which facilitated better integration and distribution of SF particles within the rubber matrix.

In contrast, SF15(SI) and SF15(SI)_R exhibited significantly lower dispersion values, rendering them unsuitable. The high SF content in SF15(SI) may have contributed to aggregation, while in SF10-CSD and SF10(SI)-CSD, calcium stearate (CSD) further promoted filler aggregation through particle-particle interactions. SF15(SI)_R, containing elevated amounts of SF and silane, compounded this issue, resulting in poor dispersion.

*Correspondence: thilinidg@sjp.ac.lk

3.9.2. GRC test

The GRC test was employed to account for the pale-yellow color of SF, which contrasts with the black color typically associated with carbon black in dispersion tests. This test is particularly relevant for compounds containing both CB and SF. As shown in Figure 4(b), the GRC test results aligned closely with the regular CB dispersion test. Trials such as SF10, SF10(SI), and SF15(SI) showed marginal improvements in dispersion compared to other formulations. While these improvements are insufficient to be deemed significant, the GRC test indicated slightly better dispersion for all trials relative to the regular CB dispersion test. These findings confirm that SF10(SI) exhibits promising dispersion properties, facilitated by silane, which enhances compatibility between SF and NR. This combination of properties underscores its potential for practical applications.

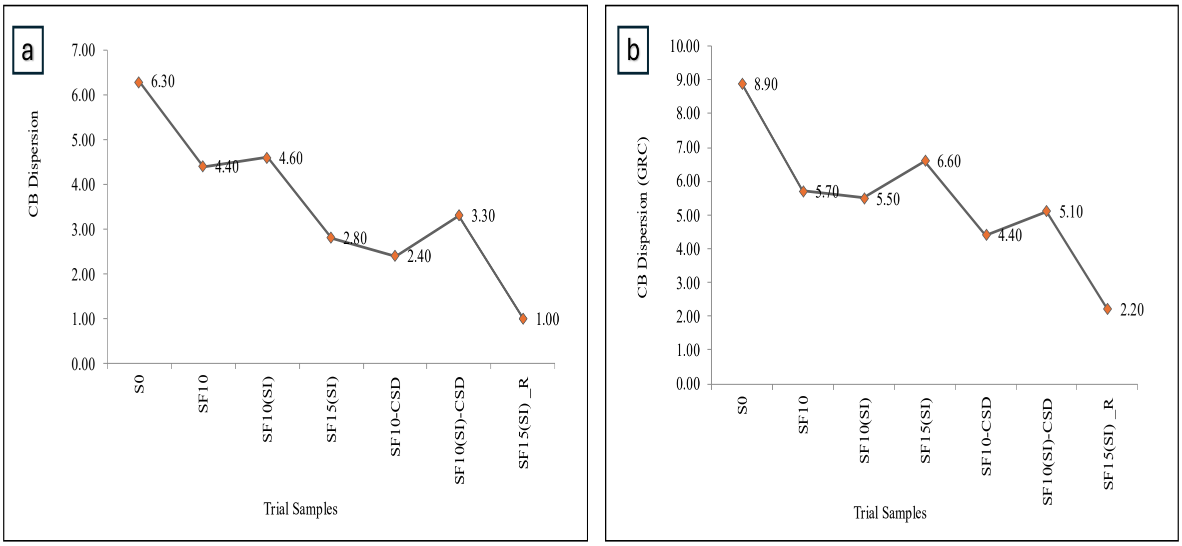

Figure 4: (a)The graph of carbon black dispersion vs. trial samples at normal condition (CB dispersion - regular test) (b) The graph of carbon black dispersion vs. trial samples at normal condition (CB dispersion - GRC test)

3.10 Spider Graph Analysis

Figure 5 shows the spider graph analysis for the SF10(SI) compared with the control sample for the parameters Tensile Strength, Hardness, Tearing Strength, Abrasion Loss, Elongation at Break, Modulus at 300% Elongation, Heat Build-Up and Probe Temperature. The SF0(SI) was selected as the possible trial among other trials. Because it shows curing, mechanical, and other properties in acceptable ranges, and especially, it shows the lowest abrasion loss compared with other trials.

When considering the mechanical properties SF10(SI) shows similar tensile strength as the control, indicating similar tensile properties. However, SF10(SI) displaying better resistance to tear propagation than the control since it has higher tear strength. Higher modulus at 300% Elongation in the SF10(SI) displays increased stiffness. SF10(SI) displays lower elongation at Break, implying reduce stretchability compared to the control. Both abrasion loss and the hardness of SF10(SI) is higher than the control reflecting improved durability. Heat buildup is higher in SF 10 along with the probe temperature indicating lower thermal properties than the control.

*Correspondence: thilinidg@sjp.ac.lk

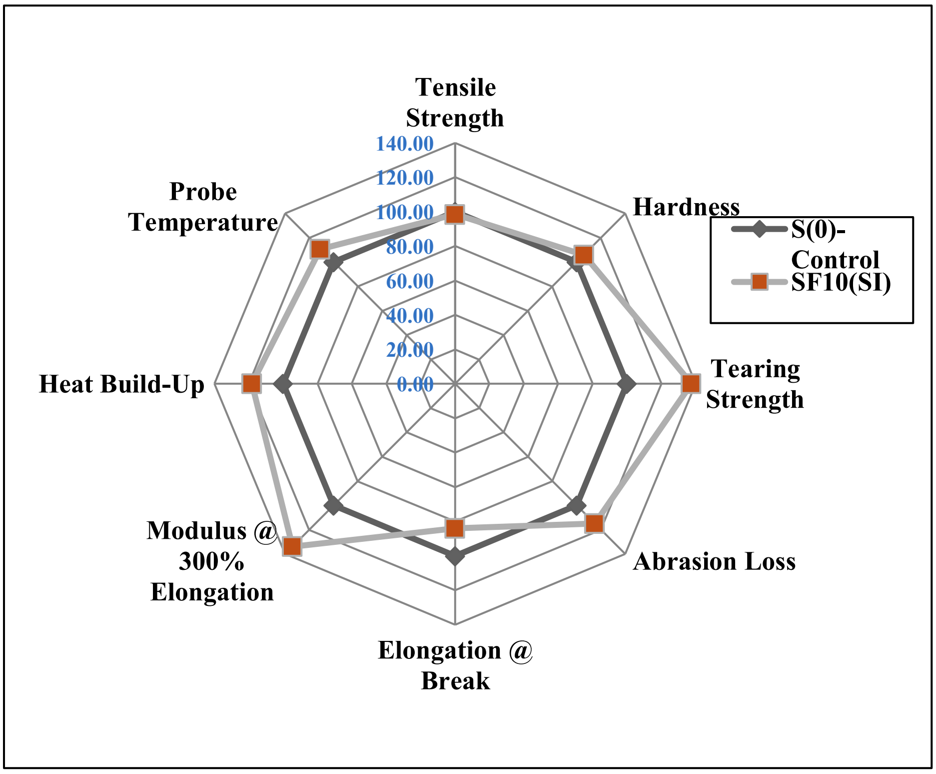

Figure 5: The spider graph analysis of SF10(SI) compared to the control(S0)* 10 phr of soya flour by replacing carbon black with silane coupling agent - SF10(SI)

4. Conclusions

Soya flour (SF) is an abundantly available biomaterial, making it a promising alternative in non-food applications, particularly in tire manufacturing. This study focused on partially replacing carbon black (CB) with SF in tire tread compounds, using natural rubber (NR) as the elastomer. Based on prior research, an initial replacement of 10 phr of CB with SF was evaluated, followed by the optimization of compatibilization techniques and SF ratios through a series of trials. SF was found to have an average moisture content of 6.74%, which, while relatively high, did not significantly compromise the overall performance of the compound. Cure properties assessed through the MDR test indicated good compatibility across all trials, except for SF10(SI), which showed a higher ML value, leading to increased mixing energy. Mechanical property evaluations revealed that tensile strength remained unaffected by the inclusion of SF. The percentage elongation at break (PEB) for SF10 exhibited minimal deviation from the control, and other samples remained within the acceptable range of 0% to -18%. Modulus at 300% elongation (M300) showed a reduction for SF10 but an improvement in all other samples. Hardness and specific gravity (SPG) values were comparable to the control, indicating that these properties were not significantly impacted by SF incorporation. Adhesion testing further highlighted the potential of SF, with SF10(SI) exhibiting superior adhesion strength compared to the control. These findings demonstrate that SF when compatibilized with silane, can successfully replace 10 phr of CB in NR-based tire tread compounds. In dynamic testing, SF10, SF10(SI), and SF15(SI) demonstrated good resilience values, while other samples showed resilience reductions of up to 18%, remaining within acceptable limits. Abrasion resistance varied, with SF10(SI) showing a 15% reduction from the control, which is acceptable, while other samples exhibited higher losses. The blooming test revealed no visible defects such as white dust or patches across all samples. SF10(SI) also showed a heat build-up value which was only 18.18% greater than the control, falling within acceptable performance limits.

This substitution provides a sustainable approach to material development in the tire industry without compromising key performance characteristics. Beyond tire applications, the results of this research open pathways for SF utilization in various other rubber products. Its successful incorporation

*Correspondence: thilinidg@sjp.ac.lk

into NR compounds suggests its potential for use in conveyor belts, automotive seals, and gaskets, vibration dampers, where similar mechanical and dynamic properties are required. Furthermore, due to the low environmental impact of SF, it could be employed in eco-friendly insulation sheets, flooring materials, and even footwear soles, contributing to greener manufacturing processes. The use of SF in these applications could significantly reduce reliance on petroleum-based fillers, promoting sustainable development across multiple industries.

5. References

Bera, A., Sarkar, K., Ganguly, D., Ghorai, S., Hore, R., Kumar, N., Amarnath, S., Chattopadhyay, S. 2024. Recent advancements in silica filled natural rubber composite: A green approach to achieve smart properties in tyre. *Journal of Polymer Research,* 31**,** 122.

Bijina, V., Jandas, P., Joseph, S., Gopu, J., Abhitha, K., John, H. 2023. Recent trends in industrial and academic developments of green tyre technology. *Polymer Bulletin,* 80**,** 8215-8244.

Chakraborty, S. 2024. Carbon black morphology and its application in elastomer and polymer matrix. *Rubber Products: Technology and Cost Optimisation***,** 53.

Fan, Y., Fowler, G. D. & Zhao, M. 2020. The past, present and future of carbon black as a rubber reinforcing filler–A review. *Journal of cleaner production,* 247**,** 119115.

Formela, K. 2021. Sustainable development of waste tires recycling technologies–recent advances, challenges and future trends. *Advanced industrial and engineering polymer research,* 4**,** 209-222.

Huang, J., Meng, Z., Peng, Y., Yang, Y., Jiang, Q., Wang, W., Chen, Z. 2022. Investigation on gas and particle emission characterization of carbon black oxidation process promoted by catalyst/ash. *Chemical Engineering Journal,* 437**,** 135015.

Innes, J. R., Siddique, N., Thompson, G., Wang, X., Coates, P., Whiteside, B., Benkreira, H., Caton-Rose, F., Lu, C., Wang, Q. 2024. The Influence of Devulcanization and Revulcanization on Sulfur Cross-Link Type/Rank: Recycling of Ground Tire Rubber. *ACS omega*.

Ismail, H., Omar, N., Othman, N. 2011. Effect of carbon black loading on curing characteristics and mechanical properties of waste tyre dust/carbon black hybrid filler filled natural rubber compounds. *Journal of Applied Polymer Science,* 121**,** 1143-1150.

Jong, L. 2005. Characterization of defatted soy flour and elastomer composites. *Journal of applied polymer science,* 98**,** 353-361.

Koriem, A. A., Abd El-Aziz, M., Salem, S. R., Hussain, A. I., Turky, G. 2023. Management of agricultural waste to manufacture biochar: An alternative reinforcing filler for carbon black in nitrile butadiene rubber composites. *Journal of Cleaner Production,* 428**,** 139360.

Neethirajan, J., Parathodika, A. R., Hu, G.H., Naskar, K. 2022. Functional rubber composites based on silica-silane reinforcement for green tire application: the state of the art. *Functional Composite Materials,* 3**,** 7.

Niranjan, R., Thakur, A. K. 2017. The toxicological mechanisms of environmental soot (black carbon) and carbon black: focus on oxidative stress and inflammatory pathways. *Frontiers in immunology,* 8**,** 763.

Petchkaew, A. 2015. Implications of non-carcinogenic PAH-free extender oils in natural rubber based tire compounds.

Pisoschi, A. M., Pop, A. 2015. The role of antioxidants in the chemistry of oxidative stress: A review. *European journal of medicinal chemistry,* 97**,** 55-74.

Rodgers, B., Waddell, W. 2005. The science of rubber compounding. *Science and technology of rubber.* Elsevier.

Rostami-Tapeh-Esmaeil, E., Kazemi, H., Ahmad, H., Morin, M., Rodrigue, D. 2023. Recycled silica as a renewable and sustainable alternative to carbon black in natural rubber foams. *Polymer International,* 72**,** 1104-1111.

**Correspondence: thilinidg@sjp.ac.lk*

Sarkawi, S. S., Kaewsakul, W., Sahakaro, K., Dierkes, W. K., Noordermeer, J. W. 2015. A review on reinforcement of natural rubber by silica fillers for use in low-rolling resistance tires. *Journal of rubber research,* 18**,** 203-233.

Schmidt, M. W., Noack, A. G. 2000. Black carbon in soils and sediments: analysis, distribution, implications, and current challenges. *Global biogeochemical cycles,* 14**,** 777-793.

Susanto, T. The effect of natural based oil as plasticizer towards physics-mechanical properties of NR-SBR blending for solid tyres. Journal of Physics: Conference Series, 2018. IOP Publishing, 012027.

Torres, B. G., Dognani, G., Da Silva Agostini, D. L., Dos Santos, R. J., Cabrera, F. C.., Aguilar, C. M. G, De Paiva, F. F. G., Teixeira, S.R., Job, A. E. 2021. Potential eco-friendly application of sugarcane bagasse ash in the rubber industry. Waste and Biomass Valorization, 12, 4599-4613.

Wypych, G. 2004. Plasticizers use and selection for specific polymers. *Handbook of plasticizers,* 1.

Xu, J., Hao, Y., Yang, Z., Li, W., Xie, W., Huang, Y., Wang, D., He, Y., Liang, Y., Matsiko, J. 2022. Rubber antioxidants and their transformation products: Environmental occurrence and potential impact. *International Journal of Environmental Research and Public Health,* 19**,** 14595.

*Correspondence: thilinidg@sjp.ac.lk